© 2019. Published by The Company of Biologists Ltd | Journal of Experimental Biology (2019) 222, jeb204651. doi:10.1242/jeb.204651

RESEARCH ARTICLE

Region-specific changes in *Mus musculus* brain size and cell composition under chronic nutrient restriction

Jimena Barbeito-Andrés[1], Emily Castro-Fonseca[2], Lily R. Qiu[3], Valeria Bernal[4], Roberto Lent[2], Mark Henkelman[3], Kenneth Lukowiak[5], Pablo M. Gleiser[6], Benedikt Hallgrimsson[7] and Paula N. Gonzalez[1,*]

ABSTRACT

Nutrition is one of the most influential environmental factors affecting the development of different tissues and organs. It is suggested that under nutrient restriction the growth of the brain is spared as a result of the differential allocation of resources from other organs. However, it is not clear whether this sparing occurs brain-wide. Here, we analyzed morphological changes and cell composition in different regions of the offspring mouse brain after maternal exposure to nutrient restriction during pregnancy and lactation. Using high-resolution magnetic resonance imaging, we found that brain regions were differentially sensitive to maternal protein restriction and exhibited particular patterns of volume reduction. The cerebellum was reduced in absolute and relative volume, while cortex volume was relatively preserved. Alterations in cell composition (examined by the isotropic fractionator method) and organization of white matter (measured by diffusor tensor images) were also region specific. These changes were not related to the metabolic rate of the regions and were only partially explained by their specific growth trajectories. This study is a first step towards understanding the mechanisms of regional brain sparing at microstructural and macrostructural levels resulting from undernutrition.

KEY WORDS: Brain sparing, Brain cortex, Cerebellum, Magnetic resonance imaging, Isotropic fractionator

INTRODUCTION

The environment experienced during early ontogeny has profound and potentially life-long effects on phenotypic variation. Nutrient restriction is a pervasive factor, with systemic effects on many tissues as well as overall body size (Figueras and Gardosi, 2011; Miller et al., 2016). Several studies in human populations suggest that brain growth is relatively protected from the effects of nutrient restriction at the expense of other parts of the body (Baker et al., 2010; Bocca-Tjeertes et al., 2014; Cohen et al., 2015; Kramer et al., 1989). Prenatal exposure to restricted nutrients and oxygen, as a consequence of maternal malnutrition or placental insufficiency, tends to result in a relatively larger head and brain (as measured by head circumference and brain volume) compared with body mass in newborns (Baker et al., 2010; Bocca-Tjeertes et al., 2014; Cox and Marton, 2009; Hunter et al., 2016). This so called 'brain sparing' effect has been observed in other organisms including rodents (Gonzalez et al., 2016) and invertebrates (Cheng et al., 2011; Lanet and Maurange, 2014). The fact that brain sparing is found in such a variety of organisms seems to reflect a pervasive plastic response by which resources are preferentially allocated to more critical organs under stressful conditions (Aiello and Wheeler, 1995). Despite this apparent sparing effect, microstructural differences have been observed in specific regions of the brain following early nutrient restriction (Antonow-Schlorke et al., 2011; Cordero et al., 1986; Durán et al., 2011; Morgane et al., 1993; Ranade et al., 2012). Consistent with this, seasonal variation in resource availability also induces differential size changes across the brain (Lázaro et al., 2018). The mechanisms that underlie these effects are unknown. This is a critical question for framing the functional consequences of environmental factors on the brain. Here, we investigated the differential response of specific brain regions to prenatal and early postnatal undernutrition in mice.

The mammalian brain can be parsed into regions that differ in function, structural properties, energetic demands and developmental trajectories (Hager et al., 2012). Differences between brain structures may account for the differential responses and susceptibility to stressful conditions. In particular, ontogenetic timing, which refers here to the sequence of structural changes throughout life, has an important role in structuring the phenotypic variation associated with changes in brain size. For instance, it was stated that those regions in which neurogenesis onset is relatively late tend to be more variable than early developing regions (Charvet et al., 2015). The pattern of growth of each region and the time and duration of exposure to a stressful factor such as undernutrition may interact to produce different results (Morgane et al., 1993, 2002). When nutrient restriction occurs throughout the period of critical brain development, those regions with more extended growth are expected to be more negatively affected because they are exposed to this stressful factor for a longer period, while brain regions that mature earlier may be less impacted. However, if nutrient restriction only occurs very early in ontogeny, brain structures that mature later may more easily compensate for those perturbations and achieve better sparing relative to their potential in the absence of the nutritional stress. Therefore, regional variation in growth trajectories is one possible explanation for regional differences in the effects of nutrient restriction on brain growth.

Alternatively, differential sparing may be associated with specific energy requirements. The energy requirements of brain areas are not homogeneous (Karbowski, 2007). Thus, one might predict that nutritional stress would more severely affect regions with higher

[1]Institute for Studies in Neuroscience and Complex Systems Studies, ENyS, CONICET, CP 1888 Buenos Aires, Argentina. [2]Institute of Biomedical Sciences, Federal University of Rio de Janeiro, Rio de Janeiro, CEP 21941-590, Brazil. [3]Mouse Imaging Centre, Hospital for Sick Children, Toronto, ON M5T 3H7, Canada. [4]Anthropology Department, School of Natural Sciences, National University of La Plata, CP 1900 Buenos Aires, Argentina. [5]Hotchkiss Brain Institute, Cumming School of Medicine, University of Calgary, Calgary, AB T2N 1N4, Canada. [6]Medical Physics Department, Bariloche Atomic Centre, Bariloche CP 8400, Río Negro, Argentina. [7]Department of Cell Biology and Anatomy, McCaig Institute for Bone and Joint Health, Alberta Children's Hospital Research Institute, University of Calgary, Calgary, AB T2N 1N4, Canada.

*Author for correspondence (paulan.gonza@gmail.com)

P.N.G., 0000-0001-6335-7363

Received 9 April 2019; Accepted 1 August 2019

Journal of Experimental Biology (2019) 222, jeb204651. doi:10.1242/jeb.204651

metabolic rates, independently of their pattern of growth. Such differences may be related to the specific metabolic requirements of the neural and glial components of the specific brain region (Karbowski, 2007). Hence, an alternative but not mutually exclusive hypothesis is that observed regional differences in sparing as a response to nutritional stress depend on regional characteristics regarding cellular composition which, in turn, may affect brain region metabolism.

Earlier work on nutrient restriction suggests that diverse mechanisms may underlie changes in brain volume. Adverse impacts on brain cell proliferation, as well as cell differentiation and growth, synaptogenesis and dendritic arborization have been reported for the hippocampus, cortex and cerebellum (Alamy and Bengelloun, 2012; Antonow-Schlorke et al., 2011; Diáz-Cintra et al., 1991; Morgane et al., 1993, 2002; Plagemann et al., 2000; Ranade et al., 2012). Because the timing of developmental processes varies between brain regions (Bandeira et al., 2009; Fu et al., 2013), the effects of nutrient restriction on microstructural components are expected to be heterogeneous. In rodents, it has been shown that neurogenesis occurs mainly prenatally for most regions, except for the cerebellum, and persists for a variable extent after birth (Aguirre, 2004; Bandeira et al., 2009; Espinosa and Luo, 2008; Fu et al., 2013). In contrast, most gliogenesis takes place after birth, although its magnitude also varies among regions (Bandeira et al., 2009). If the different cell types respond differentially to nutrient restriction, this may result in differential brain sparing.

To test the hypotheses outlined above, we experimentally induced maternal undernutrition during pregnancy and lactation in mice, as in our earlier work (Barbeito-Andrés et al., 2018; Gonzalez et al., 2016). We applied 3D imaging and well-established cell quantification methods to determine the effects of nutrient restriction on overall brain size, the size of 12 cortical and subcortical structures, and the microstructural properties of four brain structures that differ in the timing of neurogenesis and gliogenesis. Previous studies have focused on particular brain structures using a variety of techniques and experimental designs. This makes integrating results across studies difficult. This is the first study, to our knowledge, that integrates results across the scale from cell composition to the whole-organ level to understand the underlying mechanisms of regional brain changes under nutrient restriction.

MATERIALS AND METHODS

Samples and experimental design

For the nutrition experiments, 4 week old male and female C57BL/6 mice were acclimated to a 12 h light:12 h dark cycle over 4 weeks. We randomly assigned each nulliparous female to either the severe low-protein (LP) or control (C) group. At this point, we confirmed that the body mass of randomly assigned dams did not differ between experimental groups. Control animals had *ad libitum* access to a standard diet with 20% protein and 3.8 kcal g^{-1} (TD.91352, Envigo Harlan Teklad, Madison, WI, USA). In the LP group, animals were fed *ad libitum* with a low-protein (6%) isocaloric diet (TD.90016, Envigo Harlan Teklad). Further details on diet composition are presented in Table S1.

Dams were housed in pairs during the mating period in a standard cage in which a male was introduced at the beginning of every dark cycle. Males were removed from the cages every morning and females were checked for a postcoital vaginal plug; pregnant dams were then housed in single cages. Both C and LP diets were dispensed to dams from the day of pregnancy confirmation to weaning of the pups. After weaning, at postnatal day 20 (P20), pups of all groups were fed standard diet until P34. Pups usually start consuming solid food a few days before weaning. In our experimental design, standard cages were used and, therefore, pups also had access to solid food. However, before weaning (P20), pups were exposed only to the assigned diet (whether C or LP) and if they ate some kibbles, the nutritional content of the food was maintained. Based on the amount of food consumed by each dam, we estimated daily intake for each macronutrient and metabolizable energy during gestation and lactation. During these periods, LP dams consumed around one-third of the protein compared with the C group, a similar amount of fat and energy and a slightly but not significantly larger amount of carbohydrates (Table S2).

A third group of mice received a moderate low-calorie protein (LC-P) diet using the pair-feeding technique (Cesani et al., 2006). Briefly, the pair-feeding technique consists of reducing the amount of food provided to an experimental group in relation to that consumed by matched mice from the control group. From embryonic day 10.5 (E10.5), pregnant mice were fed with 80% of the daily intake of a dam in the C diet group of similar mass and at the same day of pregnancy. For this purpose, we first carried out experiments with the C group. Then, the reports on C dams were revised and the C dam that had the most similar mass at the beginning of pregnancy until E10.5 was chosen for each LC-P female. From this gestation day (E10.5) until the end of the treatment, the amount of C diet (g) consumed by the chosen C female on the corresponding day of pregnancy was taken as 100%, and this amount was reduced by 20% for the LC-P dam. Diet was weighed and disposed every day before the beginning of the dark cycle. In all cases, LC-P females ate the complete amount of food provided, suggesting that *ad libitum* intake would be greater. As expected, the LC-P dams consumed between 77% and 87% of the three components (protein, carbohydrates and fat) and energy compared with the C group dams (Table S2).

At P34, mice were anesthetized by intraperitoneal injection of a ketamine/xylazine mixture (150 mg kg^{-1} body mass ketamine and 10 mg kg^{-1} body mass xylazine) and, after confirming deep sedation through the absence of the palpebral reflex, they were perfused with 4% paraformaldehyde (PFA) through the left ventricle to fix tissues. Then, skulls were immersed into 4% PFA at 4°C for 48 h. The mice used in this study were purchased from the Animal Facility of the Veterinary Faculty, National University of La Plata, Argentina. All procedures were carried out according to the guidelines of the Canada Council on Animal Care and were reviewed and approved by the Committee for the Care and Use of Experimental Animals (CICUAL) of the Veterinary Faculty of the National University of La Plata (Protocol 42-2-14P).

Finally, to assess the hypothesis that differential effects of malnutrition on brain regions are related to region-specific growth trajectories, we analyzed an ontogenetic sample of C57BL/6 mice from which the pattern of normal postnatal growth was obtained. For this ontogenetic sample, between 1 and 2 pups per sex were randomly selected from different litters at P3 and analyzed longitudinally at P3, P5, P7, P10, P17, P23, P29 and P36 (see Qiu et al., 2018, for a detailed description of sample size for each developmental stage). Although the sample is longitudinal, some discrepancies in sample size between stages were present because of occasional scanner issues. Sample size varied between 11 and 15 animals per sex and they were obtained from approximately 10 different dams. Details on magnetic resonance imaging (MRI) acquisition for this ontogenetic sample are presented below.

Journal of Experimental Biology (2019) 222, jeb204651. doi:10.1242/jeb.204651

MRI acquisition, processing and analysis

The brains of mice from the nutritional experiment (C, LP and LC-P groups) were scanned in a 9.4 T animal MRI scanner (Bruker 9.4 T BioSpec, Experimental Imaging Centre of the University of Calgary) using the following parameters: a T2-weighted echo-gradient sequence, with TE 10 ms and field-of-view 15×15 mm and matrix size of 128×128×30. Specimens were selected to obtain a balanced distribution of sexes in each group (C: 5 males, 5 females; LP: 3 males, 4 females; LC-P: 3 males, 3 females). In order to avoid maternal effects, scanned specimens were obtained from at least 3 dams in each experimental group (number of dams: C n=6, LP n=3, LC-P n=3). Twelve brain regions of interest (ROI) were manually segmented following the Allen Reference Atlas (available at http://www.brain-map.org/; Lein et al., 2007; Dorr et al., 2008) in Avizo software (Fig. 1A) and their volume in mm^3 was obtained. These areas represent structural and functionally diverse regions that can be recognized and segmented in the MRIs with a high level of repeatability. As no significant differences between right and left sides of any ROI were found, the two hemispheres were pooled for subsequent analyses. Image processing was carried out using a blinding code for each specimen with no explicit reference to the experimental group.

We first analyzed the absolute volume of ROI to describe the main trends of morphological variation in the different regions. To this purpose, we performed a principal component analysis (PCA) on these volumes and also estimated the difference of the mean volumes between experimental groups for each ROI, using the means of the C group as the reference values; differences were expressed as the percentage change relative to the C group mean values (100%). Additionally, we defined a set of ratios by standardizing the volume of each ROI by the overall brain volume of the specimen. These variables represent relative volumes that illustrate the proportion occupied by each structure within the brain (Corruccini, 1995; Mosimann, 1970). Also, a PCA on relative volumes was performed and the percentage difference of these ratios between experimental and control groups was estimated. The analysis of relative volume captures proportions of brain components, an aspect of overall brain shape.

For both absolute and relative volumes, we performed a linear mixed model in which the volume of each ROI was the response variable, while the fixed effect was the experimental group and a random term was added for the maternal identification. An ANOVA was carried out on these models to assess the differences in ROI volumes between groups while taking into consideration the maternal effect. Finally, for those ROI in which significant differences were found, we performed pairwise differences of least-squares means. These statistical analyses were performed using the lmerTest package in R (http://www.R-project.org/).

Brain regions scale differentially with changes in brain size both along ontogeny and among specimens at the same ontogenetic stage but that differ in size (i.e. ontogenetic and static allometry; Klingenberg, 2016). Here, we tested whether the pattern of variation in the size of specific regions of the brain in the nutrient-restricted P34 mice was associated with changes in overall brain size by calculating multivariate regressions of absolute volumes of ROI on brain volume. In this case, log-transformed values were used. We assessed whether the changes in ROI volume induced by early undernutrition, particularly in the LP group, followed the allometric relationships found in the C

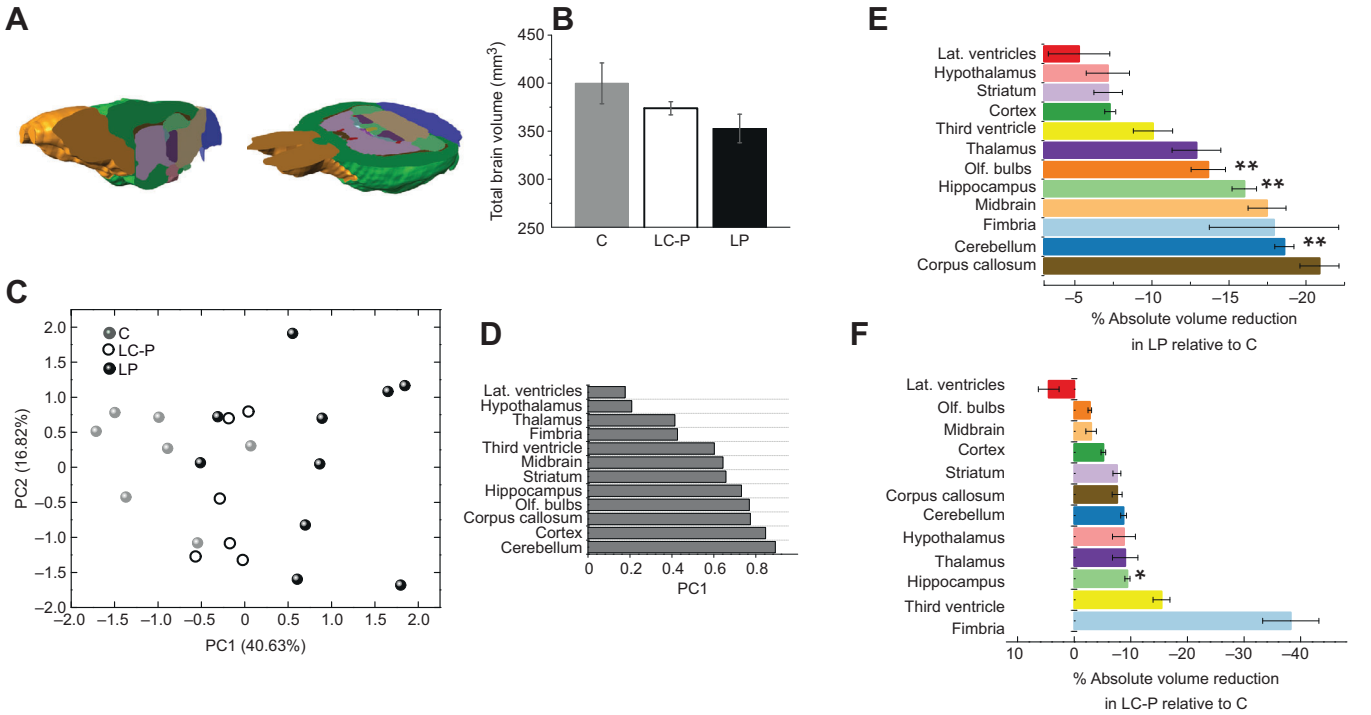

Fig. 1. Variation in absolute brain volume. (A) Regions of interest (ROI) segmented from magnetic resonance imaging (MRI). (B) Total brain volume. Means±s.d. are indicated for each experimental group: C, control group; LC-P, low-calorie protein group; LP, low-protein group. (C) Scatterplot of the first and second principal component (PC1 and PC2) of absolute volumes. (D) Loadings for each variable in PC1. (E) Mean percentage difference in absolute volumes between LP and C groups, and (F) between LC-P and C groups (*P<0.05, **P<0.01). Specimens were selected to obtain a balanced distribution of sexes in each group (C: n=10; LC-P: n=6; LP: n=7). Error bars indicate s.e.m. For more detailed statistical comparisons, see Table 1.

Journal of Experimental Biology (2019) 222, jeb204651. doi:10.1242/jeb.204651

group. With this aim, the vector of regression coefficients of the multivariate regression of C specimens was compared with the regression of the whole sample by a Pearson's product-moment correlation (Gonzalez et al., 2011). A high correlation is expected if the size changes induced by nutrient restriction follow the scaling relationships of the sample. Finally, we calculated differences between ROI volumes observed in the LP group and the expected volumes obtained through the regression performed only in C specimens. This analysis indicates how the LP group departs from C group patterns of scaling relationships within the brain.

The effect of nutrient restriction on the microstructural organization of the white matter was quantified by means of fractional anisotropy (FA; Takao et al., 2013). Higher FA values are observed along well-myelinated white matter tracts, so they are expected in voxels with healthy axonal prolongations (Kochunov et al., 2007; Takao et al., 2013). The values of FA for the 12 ROI were estimated from diffusion tensor images (DTIs) with 30 directions using DSI studio (http://dsi-studio.labsolver.org) (Yeh et al., 2013).

The animals from the ontogenetic sample were scanned *in vivo* at eight time points in a 7.0 T scanner (Varian Inc., Mouse Imaging Centre of the Hospital for Sick Children, Toronto, ON, Canada). The parameters of acquisition were: T1-weighted echo-gradient sequence, TE=5.37 ms, field-of-view=77×20×20 mm and matrix size=854×224×224, isotropic resolution 90 µm. From parcellated ROI, we first estimated the mean of each sampled age and then the percentage of the adult volume attained at each stage, taking the adult volume as 100%. More information on experimental design, acquisition parameters and image processing of this sample is available in Qiu et al. (2018).

Isotropic fractionator

Cell composition was estimated by counting the number of neuron and non-neuron cells using the isotropic fractionator (Herculano-Houzel, 2005). After scanning, brains were removed from the skull and dissected into five regions: olfactory bulbs, cortex, cerebellum, hippocampus and rest of the brain. Each region was mechanically dissociated to obtain a homogeneous suspension of isolated nuclei using a saline solution with 0.1% Triton X-100. To assess total cell number, nuclei were labeled with DAPI (4′,6-diamidino-2-phenylindole, 20 mg l^{-1}; D9542, Sigma-Aldrich) and quantified using a hemocytometer (Neubauer chamber). To estimate the fraction of nuclei that correspond to neurons, an aliquot from the suspension was immunolabeled overnight with mouse monoclonal anti-NeuN antibody (Mullen et al., 1992) (1:200 dilution in PBS; MAB377, Millipore). Then, nuclei were washed in PBS and incubated with AlexaFluor 555 anti-mouse IgG secondary antibody (1:300 dilution in PBS; A20009, Molecular Probes), in the presence of 10% normal goat serum. For each sample, NeuN-stained nuclei were counted in relation to 500 DAPI-stained nuclei and the non-neuron fraction was obtained by subtraction. Cell density was estimated as the ratio between cell number and mass (in mg) of ROI. This procedure was carried out on a subsample of specimens (C: 3 males, 3 females; LP: 3 males, 4 females; LC-P: 1 male, 1 female). Specimens derived from different dams in all groups (C: 2 dams, LP: 3 dams, LC-P: 2 dams). Differences between C and LP regarding cell composition were statistically determined by using a *t*-test and also a false discovery rate (FDR) correction for multiple comparisons (Benjamini and Hochberg, 1995). For cell counting, we used blinding codes with no reference to the experimental group.

RESULTS

Volumetric variation in the brain after nutritional restriction

Total brain volume was reduced as a consequence of maternal nutritional restriction, especially for the LP group (Fig. 1B). The brain volume in the C group was significantly larger than that of the LP group and to a lesser extent the LC-P group (F=16.52, P<0.0001; Tukey test, C versus LP P<0.0001, C versus LC-P P=0.019). The first axis of the PCA on the absolute volumes separates the LP specimens from the C group, while the LC-P specimens are in an intermediate position (Fig. 1C). The volumes of the 12 ROI had positive loadings on PC1 (Fig. 1D), being higher for those regions with large absolute volumes (e.g. cerebellum, cortex, corpus callosum, hippocampus and olfactory bulbs). As expected, the scores of the specimens on PC1 were significantly correlated with total brain volume (r=0.988, P<0.0001).

Mean differences in ROI volume between groups are presented in Fig. 1E,F, expressed as a percentage of variation between the C group and the other experimental groups (LP and LC-P). We found that the olfactory bulbs, cerebellum and hippocampus were significantly reduced in their absolute volume for the LP group, while other structures were less affected (Fig. 1E, Table 1). Similar results were obtained for the LC-P group, although the reduction in volume was only significant for the hippocampus and, in general, the magnitude of change was not as remarkable as in the LP group (Fig. 1E,F, Table 1).

We performed a PCA on the relative brain volumes to determine the response of brain proportions to nutritional stress. The first PC for the relative volumes separates the LP group from the C group to some extent, suggesting differences in brain shape. Scores from PC1 significantly correlate with total brain volume (r=0.632, P=0.007) (Fig. 2A), indicating that at least part of the shape variation depends on size changes. Loading values for PC1 reflect divergent patterns for two sets of regions: the cerebellum, midbrain, corpus callosum and olfactory bulbs exhibit positive values, while the cortex, hypothalamus and thalamus have negative values (Fig. 2B). This result indicates that some regions are relatively larger in smaller brains than in larger ones. However, only the cerebellum and the cortex displayed significant size differences (Fig. 2C, Table 1). In line with the results obtained from the PCA, the cerebellum showed a relative decrease in size in the LP group compared with the C group, while the cortex was relatively larger in the LP group (Fig. 2C). It is worth noting that relative volumes after LC-P treatment did not change significantly in any region and only a relative, although not significant, increase of lateral ventricle volume was observed (Fig. 2C).

Based on the results of the differences in regional volumes between the C and LP group, we compared their allometric patterns. The correlation between the coefficients of the multivariate regressions of the ROI volumes on total brain volume for the C group and the sample including the C and LP groups was low (r=0.336, P=0.285). This suggests that changes in the volume of the ROI related to brain size in the LP treatment differ from the normal static allometry. Additionally, we compared the ROI absolute volumes observed in LP specimens with the expected values for a brain of the same volume under normal conditions (this value was obtained using the regression formula for the C group). The volumes of the olfactory bulbs, striatum, cortex and third ventricle tended to be relatively larger in LP specimens than expected for a given brain size, while the cerebellum had a smaller volume than expected (Fig. S1). Overall, these results reinforce the idea that changes in the relative size of LP brains cannot be explained by size-related (i.e. allometric) changes only.

Journal of Experimental Biology (2019) 222, jeb204651. doi:10.1242/jeb.204651

Table 1. Results of linear mixed models for comparison of absolute and relative volumes of regions of interest (ROI) between groups

	Absolute volume		Relative volume	
Region	*F* (ANOVA)	Pairwise differences in means (*P*-values)	*F* (ANOVA)	Pairwise differences in means (*P*-values)
Olfactory bulbs	*F*=7.375	C versus LP *P*=0.009	*F*=1.336	
	P=0.02		*P*=0.285	
Cerebellum	*F*=8.630	C versus LP *P*=0.003	*F*=5.413	C versus LP *P*=0.018
	P=0.009		*P*=0.043	
Corpus callosum	*F*=1.842		*F*=0.579	
	P=0.217		*P*=0.583	
Midbrain	*F*=2.473		*F*=0.757	
	P=0.142		*P*=0.496	
Lateral ventricles	*F*=0.175		*F*=0.382	
	P=0.843		*P*=0.698	
Striatum	*F*=0.254		*F*=1.210	
	P=0.782		*P*=0.347	
Cortex	*F*=1.411		*F*=5.275	C versus LP *P*=0.011
	P=0.293		*P*=0.032	
Hypothalamus	*F*=1.192		*F*=0.460	
	P=0.324		*P*=0.647	
Third ventricle	*F*=167		*F*=0.395	
	P=0.850		*P*=0.690	
Hippocampus	*F*=14.754	C versus LP *P*=0.002,	*F*=1.903	
	P=0.005	C versus LC-P *P*=0.024	*P*=0.222	
Thalamus	*F*=1.469		*F*=0.058	
	P=0.254		*P*=0.943	
Fimbria	*F*=1.304		*F*=1.048	
	P=0.318		*P*=0.392	

Post hoc comparisons based on pairwise differences of least-squares means are also presented. C, control group; LP, low protein group; LC-P, low-calorie protein group.

Relationship between postnatal growth in ROI volume and the effect of nutrient restriction

The postnatal growth of the ROI from the ontogenetic sample of C57BL/6 mice differed in the percentage of adult volume size attained at birth as well as in the rate of growth (Fig. 3A). Some ROI, such as the cerebellum, the cortex and the hippocampus, were relatively immature at birth but showed a steep increase in volume around weaning (P23), while others exhibited a smaller size at birth and a less pronounced postnatal growth (e.g. olfactory bulbs and striatum). The hypothalamus is noteworthy because it had the largest size around birth and a fast growth rate, attaining most of its adult size in the first days of postnatal life. The thalamus also displayed an accelerated rate of growth although it had a smaller size at earlier stages. The midbrain and corpus callosum showed similar trajectories, being relatively advanced at birth and then growing at an intermediate velocity. Finally, the fimbria and ventricles had a steep perinatal growth that decelerated postnatally (Fig. 3A).

Comparison of the trajectories of normal growth and the volumetric changes induced by nutritional restriction in our experiment indicates that there is not a simple relationship between the two variables. Several regions (cerebellum, hippocampus, olfactory bulbs, thalamus, third ventricle, lateral ventricles and hypothalamus) followed a negative relationship between the percentage volume attained at birth and the percentage reduction after undernutrition in the LP group (Fig. 3B). Accordingly, larger differences between C and LP group volumes correspond to structures with small sizes at birth and for which, therefore, a large portion of their growth occurs postnatally. In contrast, those regions that attained a larger percentage of their adult volume at P0 (thalamus, hypothalamus) were less affected (Fig. 3B). However, some ROI departed from this relationship. Two of the most notable examples are the striatum and the cortex, which exhibited a large percentage of growth postnatally but were not as susceptible as other late-maturing structures to maternal undernutrition when absolute volumes were compared. In contrast, the corpus callosum and the midbrain were reduced by nutrient restriction even though they attained more than 40% of their adult size at birth (Fig. 3B). Regarding metabolic rate, we found that there was no relationship between glucose utilization and the magnitude of volumetric change per region (r=0.495, P=0.176), at least at the level examined in our experiment (Fig. 3B).

Microstructural changes

White matter tract integrity

Significant differences in FA values between C and LP groups were found for several ROI: corpus callosum (t_{15}=2.629, P=0.019), cortex (t_{15}=2.519, P=0.024), striatum (t_{15}=3.643, P=0.002), hippocampus (t_{15}=2.552, P=0.022), olfactory bulbs (t_{15}=2.209, P=0.043) and thalamus (t_{15}=3.221, P=0.006). In general, the LP group exhibited lower FA means for all regions except the fimbria (means±s.d. for each structure and group are presented in Table S3).

Cell number and composition

In the cerebellum, we found a significant reduction in cell number in LP specimens (t_{11}=3.785, P=0.015) resulting from a decrease in the number of neurons (t_{11}=4.154, P=0.01) (Fig. 4; Table S4). Along this line, the portion of cerebellar cells that were neurons was also decreased (Fig. S2) as a consequence of undernutrition but cellular density remained unaffected (Fig. 4; Table S4), suggesting that cell number accompanied ROI size reduction. In contrast, the cortex decreased in total cell number in the LP group (t_{11}=3.196, P=0.025) as a consequence of a significant reduction of non-neuron cells (t_{11}=4.889, P=0.005) and its cell density was also reduced (t_{11}=3.101, P=0.05). Contrary to the findings in the cerebellum, the ratio between neuron and non-neuron cells changed in favor of a larger proportion of neurons (Fig. 4; Fig. S2), which is related to the

Journal of Experimental Biology (2019) 222, jeb204651. doi:10.1242/jeb.204651

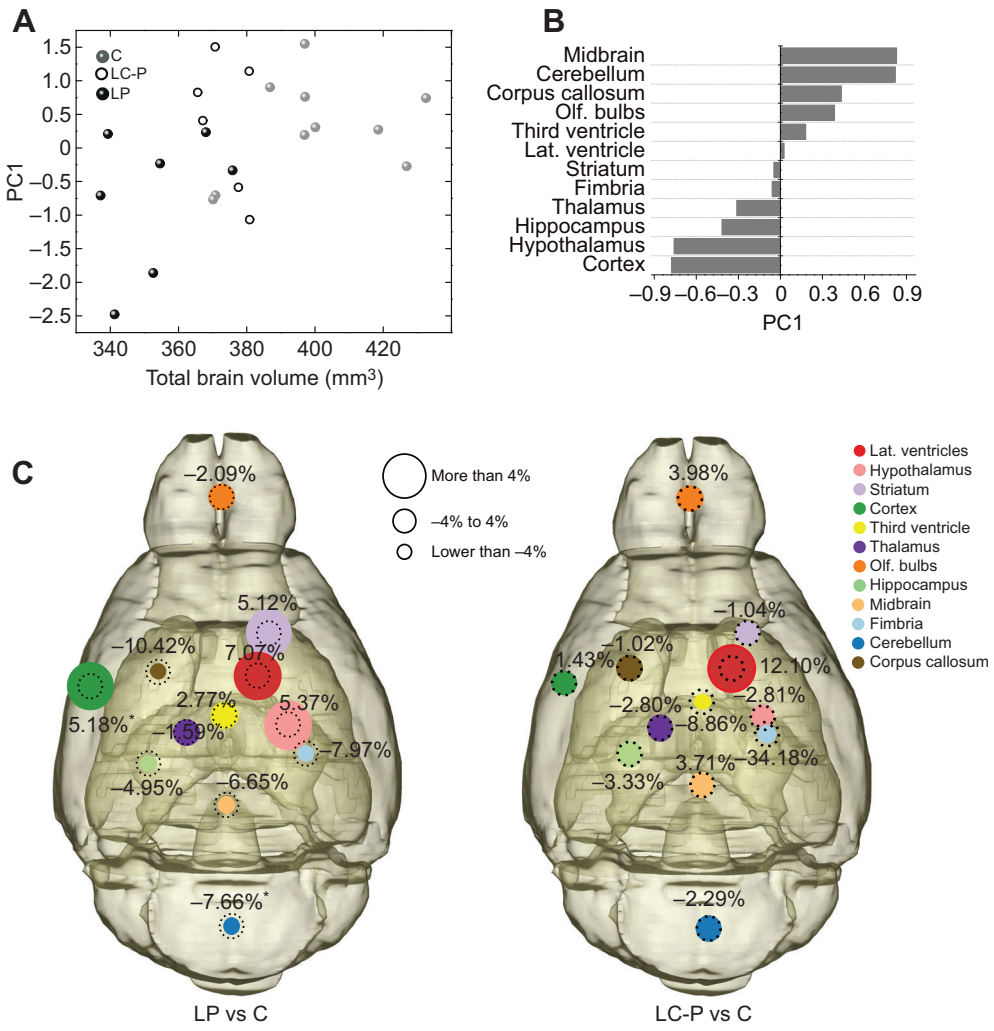

Fig. 2. Variation in relative brain volume. (A) PC1 derived from principal component analysis (PCA) on relative volumes against total brain volume. (B) Loadings for each variable in PC1. (C) Mean percentage difference in relative ROI volume (ROI/total brain) between treatment groups and C group. Circle size indicates the trend of the ROI towards a decrease, maintenance or increase of volume with associated percentages. Dashed circles are used as the reference of unchanged size compared with the C group. For more detailed statistical comparisons, see Table 1 (**P*<0.05, ***P*<0.01).

absolute decrease of non-neuron cells. In the hippocampus, cell number did not change, while in the olfactory bulbs and remaining structures (rest of the brain), there was a subtle, albeit not significant, trend towards a reduction of non-neuron cells, while neuron numbers were similar in the C and LP groups.

DISCUSSION

Our data support the hypothesis that regions of the brain are differentially sensitive to nutrient restriction during development. In a mouse model of chronic protein restriction, we found that the size of some brain regions such as the olfactory bulbs, cerebellum and hippocampus was clearly reduced, while others remained relatively unaffected. In particular, the proportion of the brain occupied by the cerebral cortex in the LP group was relatively larger than that in animals that received the standard (C) diet. Further, we found differential effects of nutritional stress on cell number and composition and white matter integrity among brain regions. Overall, these results are in line with studies that found a modular pattern of developmental plasticity in the vertebrate brain exposed to different environmental stimuli in both experimental models and wild populations (Baroncelli et al., 2010; Gonda et al., 2012; Lázaro et al., 2018). In the case of the moderate calorie–protein restriction, we found less evident structural changes, suggesting that the magnitude of the insult was not as marked as in the severe low-protein protocol.

The hypothesis that differential responses to nutritional stress result from the specific growth trajectories of each brain region was only partially supported by our data. Some structures that are relatively advanced at birth were less affected by the low-protein diet, while other ROI that complete most of their growth postnatally showed larger volume reductions. This suggests that brain development *in utero* is more highly buffered (i.e. better brain sparing) against the effects of maternal nutrient restriction than are postnatal growth and development. In a previous study we found that maternal nutrient restriction throughout pregnancy has an early effect on the size of the placenta and maternal mass, while fetal mass and head size were only affected at the end of gestation (Gonzalez et al., 2016). In contrast, the cerebellum, olfactory bulbs and hippocampus, which grow for a more extended period postnatally, were strongly affected by maternal nutritional stress. The nutritional stress applied in our model was chronic, lasting throughout pregnancy and lactation. Thus, the opportunity to catch up is probably low, even for those regions with extended growth. However, some regions did not fit the expected relationship between growth trajectories and sensitivity to protein restriction. In particular, the volume of the cortex and striatum was less affected than that of other regions despite their having a small volume at birth and a growth curve similar to that of the hippocampus. Additionally, our results do not support the hypothesis that the magnitude of effects on ROI volume is related to their metabolic demand. For

Journal of Experimental Biology (2019) 222, jeb204651. doi:10.1242/jeb.204651

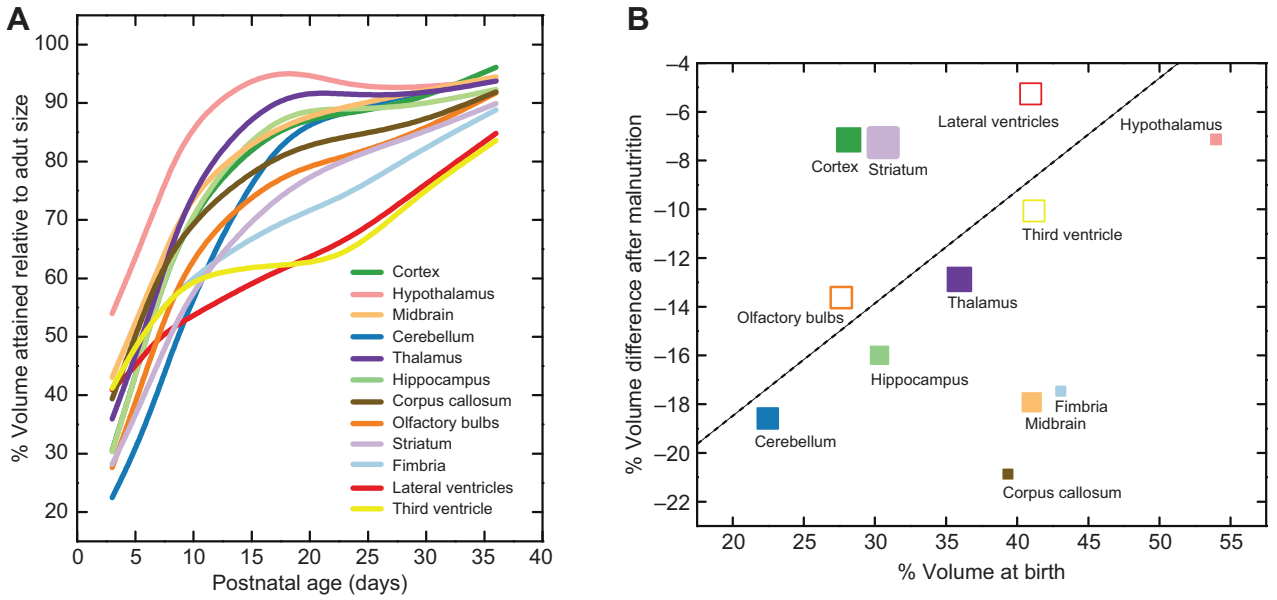

Fig. 3. Ontogenetic trajectories and adult metabolic demands of analyzed brain regions. (A) Postnatal growth of brain ROI expressed as a percentage of the mean postnatal day (P)36 volume. P3 (*n*=28), P5 (*n*=29), P7 (*n*=28), P10 (*n*=28), P17 (*n*=28), P23 (*n*=26), P29 (*n*=22) and P36 (*n*=28). Samples were obtained from a longitudinal study, in which the pups of approximately 10 dams were used at each developmental stage. (B) Relationship between the percentage of adult volume attained at birth (calculated as the difference between the volume at birth and the volume at P34 in this ontogenetic sample) and the percentage difference between C and LP groups in adult mice (these values correspond to the bars in Fig. 1E). Dashed line is only illustrative of the linear relationship for the subset of ROI for which the volume attained at birth and the difference between C and LP in adult mice correlate (cerebellum, hippocampus, olfactory bulbs, thalamus, third ventricle, lateral ventricles and hypothalamus). Symbols are sized according to their glucose utilization (Karbowski, 2007); open symbols indicate that there was no information available to determine glucose utilization for this region (in the case of olfactory bulbs) or no glucose utilization (for the ventricles).

example, as the cortex has a high metabolic rate, it would be expected to be more severely affected by nutrient restriction (Karbowski, 2007). In the same line, a recent study showed that the plastic seasonal change of brain regional volumes in shrews cannot be directly explained by the metabolic rates of different structures (Lázaro et al., 2018). It should be noted that the estimations of glucose use from different regions of the mouse brain were obtained from adult specimens. Studies on metabolic demand during human brain development have found that glucose metabolism fluctuates markedly from birth to adulthood (Chugani, 1998). In this line, we hypothesize that brain regional size variation among undernourished specimens would depend more on the metabolic demands during ontogeny than on metabolic rates of adult brains. A detailed description of the metabolic demands during the prenatal and postnatal development of the mouse brain is necessary to evaluate this alternative.

Together, our findings suggest that the cortical volume is indeed spared with prenatal and early postnatal nutrient restriction, although the underlying mechanisms remain to be elucidated. Previous studies have shown that feto-maternal blood flow can be redistributed in response to oxygen deprivation in both humans and animal models (Eixarch et al., 2008; Garcia-Canadilla et al., 2014; Miller et al., 2016; Poudel et al., 2015). Interestingly, the blood redistribution in the brain has been found to occur regionally rather than globally: the middle and anterior cerebral blood flow is first increased, while the blood flow that supplies the posterior regions is only increased when the conditions worsen (Cohen et al., 2015). The redistribution in the middle cerebral artery is particularly susceptible, which could contribute to the regional growth sparing of the cortex, given that this artery supplies a large portion of the cortex in the mouse brain (Dorr et al., 2007). As these adaptive changes have been described in humans and animal models of hypoxia during fetal development, further work is needed to test whether blood flow in brain arteries is also increased under the effect of prenatal nutritional stress and growth restriction. The regional redistribution of blood flow might, therefore, have a role in buffering the impact of environmental fluctuations on the cerebral cortex as well as in facilitating the supply of energy to meet the higher metabolic demand (Seymour et al., 2015, 2016).

We also found that the microstructural changes associated with differences in the volume induced by nutrient restriction varied across ROI. This leads us to suggest that there may be different mechanisms involved in the generation of variation in size when undernutrition occurs while the brain is developing. The number of neurons was spared compared with non-neuronal cells in all regions analyzed with the exception of the cerebellum, which showed a significant reduction in the number of neurons. This is in contrast to what was observed in the cortex, in which the proportion of neurons increased, while the number of non-neuronal cells was significantly reduced. Such a difference between the cerebellum and the cortex may relate to the developmental patterning of the cerebellum (Goldowitz and Hamre, 1998; Herculano-Houzel, 2010; Jones, 2009). In mice, neuronal number increases in the cerebellum even after the fourth week of postnatal life, while the cortex gains neurons until the second week and non-neuronal cells continue to be added even after that (Fu et al., 2013; Lyck et al., 2007). Given that cell populations in each region are dynamically modeled even in late ontogeny, it is not surprising to find remarkable changes when developmental processes are perturbed by nutritional stress. Further work based on stereological techniques that complement the isotropic fractionator method would deepen our understanding of the differential responses of specific cell populations to undernutrition.

Journal of Experimental Biology (2019) 222, jeb204651. doi:10.1242/jeb.204651

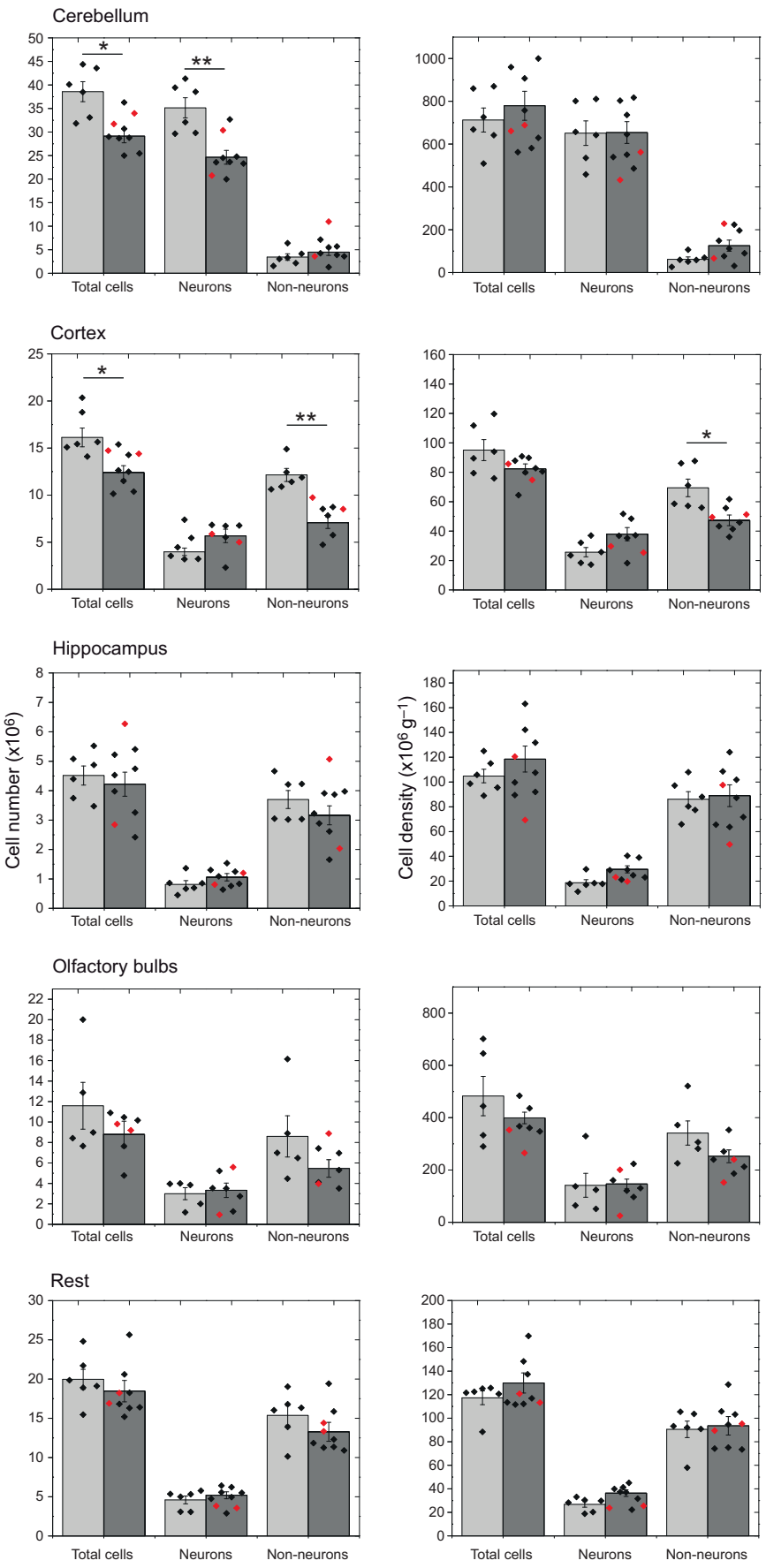

Fig. 4. Cell composition. Bars show the mean and the standard error for absolute cell number and cell density for C (light gray) and LP (dark gray) groups; diamonds represent raw data. LC-P specimens are illustrated in red although they were not included in the mean and s.e.m. estimation. Statistical differences are described in detail in Table S4 (*P<0.05, **P<0.01).

Our results also showed that some structures, such as the hippocampus and olfactory bulbs, were reduced in volume with no change in the absolute number of cells but with a significant reduction in fractional anisotropy, suggesting disrupted integrity of myelinated tracts. Such changes in fractional anisotropy have been reported previously in a different model of intrauterine growth restriction (Eixarch et al., 2012). These findings agree with postmortem studies that found a general reduction of myelin content associated with fetal growth restriction in humans (Chase et al., 1972). In particular, a reduction in hippocampus volume in prenatal growth restriction has been associated with abnormal axonal development (Miller et al., 2014, 2016). Consequently, it is expected that such changes impact cognitive processes that are dependent on hippocampal function.

This work provides evidence for the potential of non-invasive imaging methods to study the structural consequences of growth restriction due to undernutrition, which may have important applications in human studies and in clinical practice (Isaacs, 2013). Although linear extrapolations of our results to other mammals should take into account species-specific differences, it is known that the sequence of key events of brain development is highly conserved (Clancy et al., 2001). In our model, maternal undernutrition was applied during the whole of fetal intrauterine life and the lactation period following birth. Thus, the nutritional stress applied to the maternal mouse corresponds to the temporal range occurring prenatally in other mammals, including humans.

The extent to which differential growth within the brain constrains the responses to environmental stress is an open question. A strong relationship between the timing of neurogenesis and variation in the size of brain regions has been postulated, suggesting that those structures whose cell progenitors differentiate later will be larger when brain size increases (Finlay and Darlington, 1995). Previous work has challenged the validity of this hypothesis (Weisbecker, 2009) and here we showed that developmental plasticity can alter the scaling relationship as a consequence of trait-specific responses even to systemic external inputs. This is remarkable in the case of the cortex and cerebellum, which exhibited disparate responses to nutrient restriction. Overall, our findings represent a first step towards understanding developmental mechanisms that modulate the differential response of brain regions to nutritional stress.

Acknowledgements
We would like to acknowledge Dr Jeffrey F. Dunn, David Rushforth and Tadeusz Foniok for their help with MRI acquisition (University of Calgary). We thank Raveena Dhaliwal for providing scripts for image processing (University of Calgary) and Dr Fabian Nishida for his help with tissue fixation (Facultad de Ciencias Veterinarias, Universidad Nacional de La Plata). The experiments were conducted at the animal facility of the Faculty of Medicine at Universidad Nacional de La Plata, supervised by Dr Laura Andrini, Dr Marcela García and Dr Ana Lía Errecalde (Cátedra de Citología, Histología y Embriología A, Universidad Nacional de La Plata).

Competing interests
The authors declare no competing or financial interests.

Author contributions
Conceptualization: J.B.-A., V.B., K.L., B.H., P.N.G.; Methodology: J.B.-A.; Formal analysis: J.B.-A., P.M.G., P.N.G.; Investigation: J.B.-A., E.C.-F., L.R.Q., R.L., M.H., P.N.G.; Resources: R.L., M.H., P.M.G., B.H.; Writing - original draft: J.B.-A., E.C.-F., L.R.Q., V.B., R.L., M.H., P.M.G., B.H., P.N.G.; Writing - review & editing: J.B.-A., K.L., B.H., P.N.G.; Supervision: P.M.G., P.N.G.; Project administration: P.N.G.; Funding acquisition: B.H., P.N.G.

Funding
This study was supported by grants from Consejo Nacional de Investigaciones Científicas y Técnicas (National Research Council of Argentina; PIP 0603), Agencia de Promoción Científica y Tecnológica (National Agency for the Promotion of Science and Technology; PICT 1810: and Universidad Nacional de La Plata (N787). Part of the work was done in Brazil with funds from the Rio de Janeiro Foundation for the Support of Science (Fundação de Amparo à Pesquisa do Estado do Rio de Janeiro, FAPERJ) and the National Council for Research (Conselho Nacional de Desenvolvimento Científico e Tecnológico, CNPq) to R.L.

Data availability
Data are available from the figshare repository: doi:10.6084/m9.figshare.9730136

Supplementary information
Supplementary information available online at
http://jeb.biologists.org/lookup/doi/10.1242/jeb.204651.supplemental

References
Aguirre, A. (2004). Postnatal neurogenesis and gliogenesis in the olfactory bulb from NG2-expressing progenitors of the subventricular zone. *J. Neurosci.* **24**, 10530-10541. doi:10.1523/JNEUROSCI.3572-04.2004

Aiello, L. C. and Wheeler, P. (1995). The expensive-tissue hypothesis: the brain and the digestive system in human and primate evolution. *Curr. Anthropol.* **36**, 199-221. doi:10.1086/204350

Alamy, M. and Bengelloun, W. A. (2012). Malnutrition and brain development: an analysis of the effects of inadequate diet during different stages of life in rat. *Neurosci. Biobehav. Rev.* **36**, 1463-1480. doi:10.1016/j.neubiorev.2012.03.009

Antonow-Schlorke, I., Schwab, M., Cox, L. A., Li, C., Stuchlik, K., Witte, O. W., Nathanielsz, P. W. and McDonald, T. J. (2011). Vulnerability of the fetal primate brain to moderate reduction in maternal global nutrient availability. *Proc. Natl. Acad. Sci. USA* **108**, 3011-3016. doi:10.1073/pnas.1009838108

Baker, J., Workman, M., Bedrick, E., Frey, M. A., Hurtado, M. and Pearson, O. (2010). Brains versus brawn: an empirical test of barkers brain sparing model. *Am. J. Hum. Biol.* **22**, 206-215. doi:10.1002/ajhb.20979

Bandeira, F., Lent, R. and Herculano-Houzel, S. (2009). Changing numbers of neuronal and non-neuronal cells underlie postnatal brain growth in the rat. *Proc. Natl. Acad. Sci. USA* **106**, 14108-14113. doi:10.1073/pnas.0804650106

Barbeito-Andrés, J., Gleiser, P. M., Bernal, V., Hallgrímsson, B. and Gonzalez, P. N. (2018). Brain structural networks in mouse exposed to chronic maternal undernutrition. *Neuroscience* **380**, 14-26. doi:10.1016/j.neuroscience.2018.03.049

Baroncelli, L., Braschi, C., Spolidoro, M., Begenisic, T., Sale, A. and Maffei, L. (2010). Nurturing brain plasticity: impact of environmental enrichment. *Cell Death Differ.* **17**, 1092-1103. doi:10.1038/cdd.2009.193

Benjamini, Y. and Hochberg, Y. (1995). Controlling the false discovery rate: a practical and powerful approach to multiple testing. *J. R. Stat. Soc. Ser. B* **57**, 289-300. doi:10.1111/j.2517-6161.1995.tb02031.x

Bocca-Tjeertes, I., Bos, A., Kerstjens, J., de Winter, A. and Reijneveld, S. (2014). Symmetrical and asymmetrical growth restriction in preterm-born children. *Pediatrics* **133**, e650-e656. doi:10.1542/peds.2013-1739

Cesani, M. F., Orden, A. B., Oyhenart, E. E., Zucchi, M., Muñe, M. C. and Pucciarelli, H. M. (2006). Growth of functional cranial components in rats submitted to intergenerational undernutrition. *J. Anat.* **209**, 137-147. doi:10.1111/j.1469-7580.2006.00603.x

Charvet, C. J., Cahalane, D. J. and Finlay, B. L. (2015). Systematic, cross-cortex variation in neuron numbers in rodents and primates. *Cereb. Cortex* **25**, 147-160. doi:10.1093/cercor/bht214

Chase, H. P., Welch, N. N., Dabiere, C. S., Vasan, N. S. and Butterfield, L. J. (1972). Alterations in human brain biochemistry following intrauterine growth retardation. *Pediatrics* **50**, 403-411.

Cheng, L. Y., Bailey, A. P., Leevers, S. J., Ragan, T. J., Driscoll, P. C. and Gould, A. P. (2011). Anaplastic lymphoma kinase spares organ growth during nutrient restriction in Drosophila. *Cell* **146**, 435-447. doi:10.1016/j.cell.2011.06.040

Chugani, H. T. (1998). A critical period of brain development: studies of cerebral glucose utilization with PET. *Prev. Med.* **188**, 184-188. doi:10.1006/pmed.1998.0274

Clancy, B., Darlington, R. B. and Finlay, B. L. (2001). Translating developmental time across mammalian species. *Neuroscience* **105**, 7-17. doi:10.1016/S0306-4522(01)00171-3

Cohen, E., Baerts, W. and van Bel, F. (2015). Brain-sparing in intrauterine growth restriction: considerations for the neonatologist. *Neonatology* **108**, 269-276. doi:10.1159/000438451

Cordero, M. E., Trejo, M., García, E., Barros, T., Rojas, A. M. and Colombo, M. (1986). Dendritic development in the neocortex of adult rats following a maintained prenatal and/or early postnatal life undernutrition. *Early Hum. Dev.* **14**, 245-258. doi:10.1016/0378-3782(86)90186-6

Corruccini, R. S. (1995). Of ratios and rationality. *Am. J. Phys. Anthropol.* **96**, 189-191. doi:10.1002/ajpa.1330960209

Cox, P. and Marton, T. (2009). Pathological assessment of intrauterine growth restriction. *Best Pract. Res. Clin. Obstet. Gynaecol.* **23**, 751-764. doi:10.1016/j.bpobgyn.2009.06.006

Diáz-Cintra, S., Cintra, L., Galván, A., Aquilar, A., Kemper, T. and Morgane, P. J. (1991). Effects of prenatal protein deprivation on the postnatal development of granule cell in the fascia dentate. *J. Comp. Neurol.* **310**, 356-364. doi:10.1002/cne.903100306

Dorr, A., Sled, J. G. and Kabani, N. (2007). Three-dimensional cerebral vasculature of the CBA mouse brain: a magnetic resonance imaging and micro computed tomography study. *Neuroimage* **35**, 1409-1423. doi:10.1016/j.neuroimage.2006.12.040

Dorr, A., Lerch, J. P., Spring, S., Kabani, N. and Henkelman, R. M. (2008). High resolution three-dimensional brain atlas using an average magnetic resonance image of 40 adult C57Bl/6J mice. *Neuroimage* **42**, 60-69. doi:10.1016/j.neuroimage.2008.03.037

Durán, P., Miranda-Anaya, M., Romero-Sánchez, M. D. J., Mondragón-Soto, K., Granados-Rojas, L. and Cintra, L. (2011). Time-place learning is altered by perinatal low-protein malnutrition in the adult rat. *Nutr. Neurosci.* **14**, 145-150. doi:10.1179/147683011X13009738172567

Eixarch, E., Meler, E., Iraola, A., Illa, M., Crispi, F., Hernandez-Andrade, E., Gratacos, E. and Figueras, F. (2008). Neurodevelopmental outcome in 2-year-old infants who were small-for-gestational age term fetuses with cerebral blood flow redistribution. *Ultrasound Obstet. Gynecol.* **32**, 894-899. doi:10.1002/uog.6249

Eixarch, E., Batalle, D., Illa, M., Muñoz-Moreno, E., Arbat-Plana, A., Amat-Roldan, I., Figueras, F. and Gratacós, E. (2012). Neonatal neurobehavior and diffusion MRI changes in brain reorganization due to intrauterine growth restriction in a rabbit model. *PLoS ONE* **7**, e31497. doi:10.1371/journal.pone.0031497

Espinosa, J. S. and Luo, L. (2008). Timing neurogenesis and differentiation: insights from quantitative clonal analyses of cerebellar granule cells. *J. Neurosci.* **28**, 2301-2312. doi:10.1523/JNEUROSCI.5157-07.2008

Figueras, F. and Gardosi, J. (2011). Intrauterine growth restriction: new concepts in antenatal surveillance, diagnosis, and management. *Am. J. Obstet. Gynecol.* **204**, 288-300. doi:10.1016/j.ajog.2010.08.055

Finlay, B. L. and Darlington, R. B. (1995). Linked regularities in the development and evolution of mammalian brains. *Science* **268**, 1578-1584. doi:10.1126/science.7777856

Fu, Y. H., Rusznák, Z., Herculano-Houzel, S., Watson, C. and Paxinos, G. (2013). Cellular composition characterizing postnatal development and maturation of the mouse brain and spinal cord. *Brain Struct. Funct.* **218**, 1337-1354. doi:10.1007/s00429-012-0462-x

Garcia-Canadilla, P., Rudenick, P. A., Crispi, F., Cruz-Lemini, M., Palau, G., Camara, O., Gratacos, E. and Bijens, B. H. (2014). A computational model of the fetal circulation to quantify blood redistribution in intrauterine growth restriction. *PLoS Comput. Biol.* **10**, e1003667. doi:10.1371/journal.pcbi.1003667

Goldowitz, D. and Hamre, K. (1998). The cells and molecules that make a cerebellum. *Trends Neurosci.* **21**, 375-382. doi:10.1016/S0166-2236(98)01313-7

Gonda, A., Välimäki, K., Herczeg, G. and Merilä, J. (2012). Brain development and predation: plastic responses depend on evolutionary history. *Biol. Lett.* **8**, 249-252. doi:10.1098/rsbl.2011.0837

Gonzalez, P. N., Perez, S. I. and Bernal, V. (2011). Ontogenetic allometry and cranial shape diversification among human populations from South America. *Anat. Rec.* **294**, 1864-1874. doi:10.1002/ar.21454

Gonzalez, P. N., Gasperowicz, M., Barbeito-Andrés, J., Klenin, N., Cross, J. C. and Hallgrímsson, B. (2016). Chronic protein restriction in mice impacts placental function and maternal body weight before fetal growth. *PLoS ONE* **11**, e0152227. doi:10.1371/journal.pone.0152227

Hager, R., Lu, L., Rosen, G. D. and Williams, R. W. (2012). Genetic architecture supports mosaic brain evolution and independent brain-body size regulation. *Nat. Commun.* **3**, 1079. doi:10.1038/ncomms2086

Herculano-Houzel, S. (2005). Isotropic fractionator: a simple, rapid method for the quantification of total cell and neuron numbers in the brain. *J. Neurosci.* **25**, 2518-2521. doi:10.1523/JNEUROSCI.4526-04.2005

Herculano-Houzel, S. (2010). Coordinated scaling of cortical and cerebellar numbers of neurons. *Front. Neuroanat.* **4**, 12. doi:10.3389/fnana.2010.00012

Hunter, D. S., Hazel, S. J., Kind, K. L., Owens, J. A., Pitcher, J. B. and Gatford, K. L. (2016). Programming the brain: common outcomes and gaps in knowledge from animal studies of IUGR. *Physiol. Behav.* **164**, 233-248. doi:10.1016/j.physbeh.2016.06.005

Isaacs, E. B. (2013). Neuroimaging, a new tool for investigating the effects of early diet on cognitive and brain development. *Front. Hum. Neurosci.* **7**, 445. doi:10.3389/fnhum.2013.00445

Jones, E. G. (2009). The origins of cortical interneurons: mouse versus monkey and human. *Cereb. Cortex* **19**, 1953-1956. doi:10.1093/cercor/bhp088

Karbowski, J. (2007). Global and regional brain metabolic scaling and its functional consequences. *BMC Biol.* **5**, 1-11. doi:10.1186/1741-7007-5-18

Klingenberg, C. P. (2016). Size, shape and form: concepts of allometry in geometric morphometrics. *Dev. Genes Evol.* **226**, 113-137. doi:10.1007/s00427-016-0539-2

Kochunov, P., Thompson, P. M., Lancaster, J. L., Bartzokis, G., Smith, S., Coyle, T., Royall, D. R., Laird, A. and Fox, P. T. (2007). Relationship between white matter fractional anisotropy and other indices of cerebral health in normal aging: tract-based spatial statistics study of aging. *Neuroimage* **35**, 478-487. doi:10.1016/j.neuroimage.2006.12.021

Kramer, M. S., McLean, F. H., Olivier, M., Willis, D. M. and Usher, R. H. (1989). Body proportionality and head and length "sparing" in growth-retarded neonates: a critical reappraisal. *Pediatrics* **84**, 717-723.

Lanet, E. and Maurange, C. (2014). Building a brain under nutritional restriction: Insights on sparing and plasticity from Drosophila studies. *Front. Physiol.* **5**, 1-9. doi:10.3389/fphys.2014.00117

Lázaro, J., Hertel, M., Sherwood, C. C., Muturi, M. and Dechmann, D. K. N. (2018). Profound seasonal changes in brain size and architecture in the common shrew. *Brain Struct. Funct.* **223**, 2823-2840. doi:10.1007/s00429-018-1666-5

Lein, E. S., Hawrylycz, M. J., Ao, N., Ayres, M., Bensinger, A., Bernard, A., Boe, A. F., Boguski, M. S., Brockway, K. S., Byrnes, E. J. et al. (2007). Genome-wide atlas of gene expression in the adult mouse brain. *Nature* **445**, 168-176. doi:10.1038/nature05453

Lyck, L., Krøigård, T. and Finsen, B. (2007). Unbiased cell quantification reveals a continued increase in the number of neocortical neurones during early post-natal development in mice. *Eur. J. Neurosci.* **26**, 1749-1764. doi:10.1111/j.1460-9568.2007.05763.x

Miller, S. L., Yawno, T., Alers, N. O., Castillo-Melendez, M., Supramaniam, V. G., Van Zyl, N., Sabaretnam, T., Loose, J. M., Drummond, G. R., Walker, D. W. et al. (2014). Antenatal antioxidant treatment with melatonin to decrease newborn neurodevelopmental deficits and brain injury caused by fetal growth restriction. *J. Pineal Res.* **56**, 283-294. doi:10.1111/jpi.12121

Miller, S. L., Huppi, P. S. and Mallard, C. (2016). The consequences of fetal growth restriction on brain structure and neurodevelopmental outcome. *J. Physiol.* **594**, 807-823. doi:10.1113/JP271402

Morgane, P. J., Austin-LaFrance, R., Bronzino, J., Tonkiss, J., Díaz-Cintra, S., Cintra, L., Kemper, T. and Galler, J. R. (1993). Prenatal malnutrition and development of the brain. *Neurosci. Biobehav. Rev.* **17**, 91-128. doi:10.1016/S0149-7634(05)80234-9

Morgane, P. J., Mokler, D. J. and Galler, J. R. (2002). Effects of prenatal protein malnutrition on the hippocampal formation. *Neurosci. Biobehav. Rev.* **26**, 471-483. doi:10.1016/S0149-7634(02)00012-X

Mosimann, J. E. (1970). Size allometry: size and shape variables with characterizations of the lognormal and generalized gamma distributions. *J. Am. Stat. Assoc.* **65**, 930-945. doi:10.1080/01621459.1970.10481136

Mullen, R. J., Buck, C. R. and Smith, A. M. (1992). NeuN, a neuronal specific nuclear protein in vertebrates. *Development* **116**, 201-211.

Plagemann, A., Harder, T., Rake, A., Melchior, K., Rohde, W. and Dörner, G. (2000). Hypothalamic nuclei are malformed in weanling offspring of low protein malnourished rat dams. *J. Nutr.* **130**, 2582-2589. doi:10.1093/jn/130.10.2582

Poudel, R., McMillen, I. C., Dunn, S. L., Zhang, S. and Morrison, J. L. (2015). Impact of chronic hypoxemia on blood flow to the brain, heart, and adrenal gland in the late-gestation IUGR sheep fetus. *Am. J. Physiol. Regul. Integr. Comp. Physiol.* **308**, R151-R162. doi:10.1152/ajpregu.00036.2014

Qiu, L. R., Fernandes, D. J., Szulc-Lerch, K. U., Dazai, J., Nieman, B. J., Turnbull, D. H., Foster, J. A., Palmert, M. R. and Lerch, J. P. (2018). Mouse MRI shows brain areas relatively larger in males emerge before those larger in females. *Nat. Commun.* **9**, 2615. doi:10.1038/s41467-018-04921-2

Ranade, S. C., Sarfaraz Nawaz, M., Kumar Rambtla, P., Rose, A. J., Gressens, P. and Mani, S. (2012). Early protein malnutrition disrupts cerebellar development and impairs motor coordination. *Br. J. Nutr.* **107**, 1167-1175. doi:10.1017/S0007114511004119

Seymour, R. S., Angove, S. E., Snelling, E. P. and Cassey, P. (2015). Scaling of cerebral blood perfusion in primates and marsupials. *J. Exp. Biol.* **218**, 2631-2640. doi:10.1242/jeb.124826

Seymour, R. S., Bosiocic, V. and Snelling, E. P. (2016). Fossil skulls reveal that blood flow rate to the brain increased faster than brain volume during human evolution. *R. Soc. open sci.* **3**, 160305. doi:10.1098/rsos.160305

Takao, H., Hayashi, N. and Ohtomo, K. (2013). White matter microstructure asymmetry: effects of volume asymmetry on fractional anisotropy asymmetry. *Neuroscience* **231**, 1-12. doi:10.1016/j.neuroscience.2012.11.038

Weisbecker, V. (2009). Why "late equals large" does not work. *Neuroscience* **164**, 1648-1652. doi:10.1016/j.neuroscience.2009.09.027

Yeh, F.-C., Verstynen, T. D., Wang, Y., Fernández-Miranda, J. C. and Tseng, W.-Y. I. (2013). Deterministic diffusion fiber tracking improved by quantitative anisotropy. *PLoS ONE* **8**, e80713. doi:10.1371/journal.pone.0080713

	C diet	LP diet
Casein (g/kg)	230	69
DL-Methionine (g/kg)	3	0.9
Sucrose (g/kg)	431.7	571.8
Corn starch (g/kg)	200	200
Corn oil (g/kg)	52.3	53.9
Cellulose (g/kg)	37.86	57.82
Vitamin mix (g/kg)	10	10
Ethoxyquin (g/kg)	0.01	0.01
Mineral mix (g/kg)	13.37	13.37
Calcium phosphate (g/kg)	16.66	21.6
Calcium carbonate (g/kg)	5.1	1.6
Total energy from protein (kcal/g)	1.0962	0.3294
Total energy from carbohydrate (kcal/g)	2.5256	3.0996
Total energy from fat (kcal/g)	0.5115	0.5115
Total energy (kcal/g)	4.1333	3.9405
Metabolizable energy from protein (kcal/g)	0.8208	0.247
Metabolizable energy from carbohydrate (kcal/g)	2.4852	3.0552
Metabolizable energy from fat (kcal/g)	0.494	0.4978
Metabolizable energy (kcal/g)	3.8	3.8

Table S1. Composition of control (C) and low protein (LP) diets.

	C	LC-P	LP
	Protein intake (g/d)		
E0.5-E9.5	0.652 ±0.100	0.602 ±0.005	0.190 ±0.027
E10.5-Birth	0.758 ±0.083	0.633 ±0.029	0.265 ±0.025
P1-P10	1.151 ±0.496	0.887 ±0.084	0.325 ±0.047
P11-P18	1.486 ±0.194	1.299 ±0.067	0.441 ±0.068
	Carbohydrate intake (g/d)		
E0.5-E9.5	1.977 ±0.305	1.828 ±0.015	2.353 ±0.334
E10.5-Birth	2.299 ±0.250	1.92 ±0.089	3.289 ±0.310
P1-P10	3.493 ±0.150	2.692 ±0.255	4.033 ±0.582
P11-P18	4.510 ±0.589	3.943 ±0.203	5.459 ±0.843
	Fat intake (g/d)		
E0.5-E9.5	0.177 ±0.027	0.163 ±0.001	0.171 ±0.024
E10.5-Birth	0.205 ±0.022	0.171 ±0.008	0.239 ±0.023
P1-P10	0.311 ±0.013	0.24 ±0.023	0.293 ±0.042
P11-P18	0.403 ±0.053	0.352 ±0.018	0.397 ±0.061
	Energy intake (kcal/d)		
E0.5-E9.5	12.198 ±1.881	11.277 ±0.094	11.828 ±1.679
E10.5-Birth	14.184 ±1.545	11.8465 ±0.549	16.531 ±1.558
P1-P10	21.546 ±0.928	16.604 ±1.574	20.273 ±2.923
P11-P18	27.826 ±3.635	24.323 ±1.250	27.442 ±4.237

Table S2. Daily intake of macronutrients and metabolizable energy for each experimental group (C: control; LC-P: low calorie protein; LP: low protein). Means and SD are indicated.

	C	LC-P	LP
Olfactory bulbs	0.279 ± 0.009	0.271 ± 0.015	0.262 ± 0.022
Cerebellum	0.233 ± 0.014	0.227 ± 0.010	0.225 ± 0.013
Corpus callosum	0.340 ± 0.026	0.334 ± 0.038	0.306 ± 0.027
Midbrain	0.256 ± 0.020	0.257 ± 0.015	0.242 ± 0.009
Lateral ventricles	0.251 ± 0.013	0.258 ± 0.010	0.244 ± 0.022
Striatum	0.242 ± 0.012	0.247 ± 0.015	0.219 ± 0.014
Cortex	0.223 ± 0.012	0.219 ± 0.010	0.211 ± 0.006
Hypothalamus	0.246 ± 0.016	0.256 ± 0.017	0.237 ± 0.016
Thrid ventricle	0.216 ± 0.013	0.213 ± 0.016	0.211 ± 0.016
Hippocampus	0.239 ± 0.011	0.241 ± 0.008	0.225 ± 0.011
Thalamus	0.283 ± 0.018	0.287 ± 0.012	0.258 ± 0.012
Fimbria	0.278 ± 0.027	0.297 ± 0.051	0.283 ± 0.051

Table S3. FA in each ROI per group. Mean ± SD are presented.

	Cell composition			Cell density		
	Total cell number	Neurons number	Non-neurons number	Total cell density	Neurons density	Non-neurons density
Region	t (p-value)	t (p-value)	t (p-value)	t (p-value)	t (p-value)	t (p-value)
Olfactory bulbs	1.093 (0.510)	-0.363 (0.882)	1.452 (0.312)	0.969 (0.451)	-0.093 (0.967)	1.522 (0.277)
Cortex	3.196 (0.025)	-1.014 (0.562)	4.889 (0.005)	1.690 (0.451)	-2.134 (0.098)	3.101 (0.050)
Rest	0.779 (0.551)	-0.882 (0.882)	1.209 (0.312)	-1.171 (0.451)	-2.535 (0.070)	-0.283 (0.802)
Cerebellum	3.785 (0.015)	4.154 (0.010)	-1.061 (0.312)	-0.743 (0.451)	-0.042 (0.967)	-2.140 (0.140)
Hippocampus	0.550 (0.593)	-1.375 (0.493)	-1.198 (0.312)	-1.101 (0.451)	-2.845 (0.070)	-0.257 (0.802)

Table S4. t-test results for comparisons of cell number and density between C and LP. P-values, shown in parentheses, are corrected for multiple comparisons (FDR).

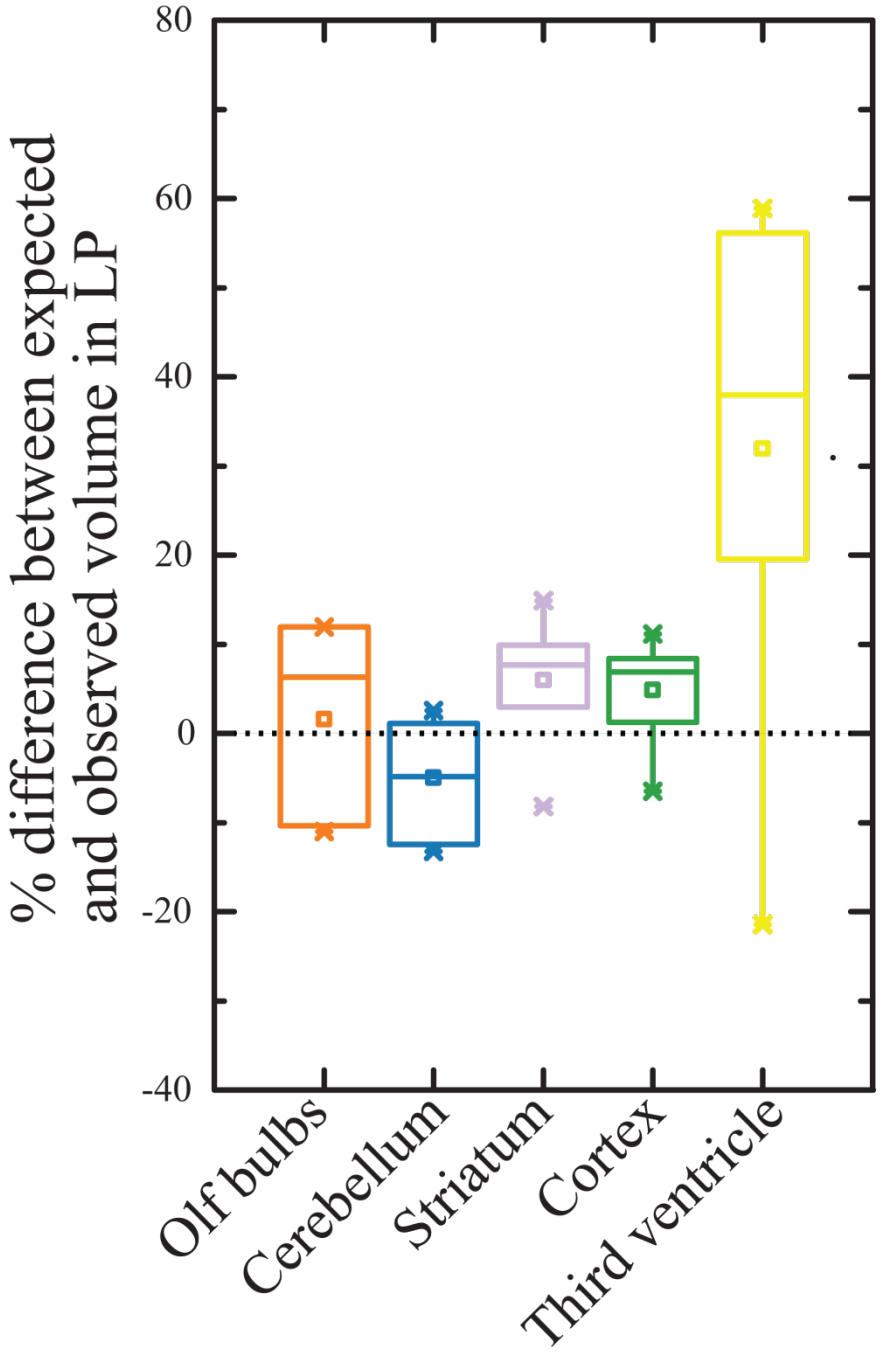

Figure S1. Volume difference (%) between expected values (for a given brain volume in C conditions) and the observed values in LP specimens.

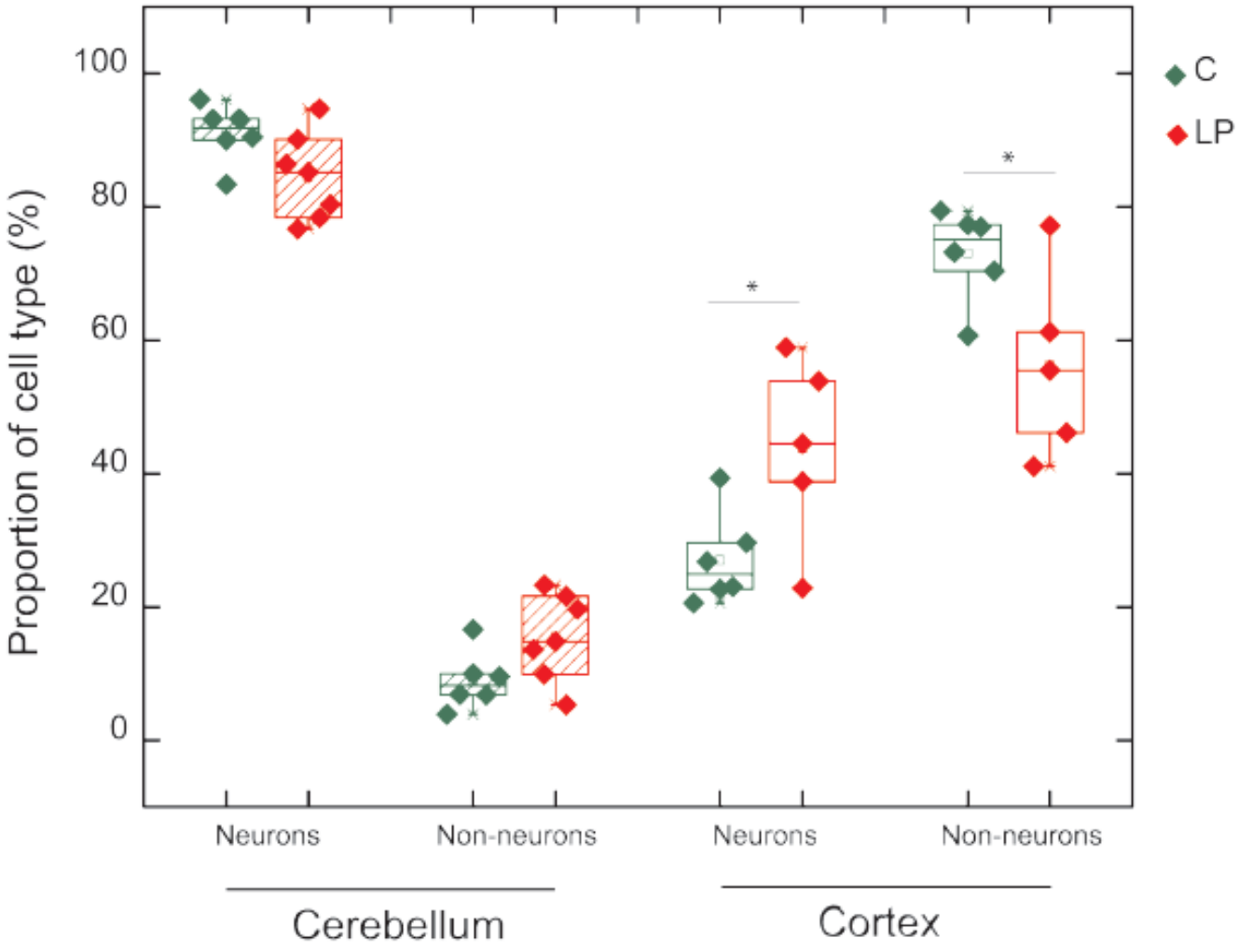

Figure S2. Box-plot showing the proportion of neuron and non-neuron cells for the cortex and the cerebellum. Significant differences between groups after t-test are depicted **p<0.01, *p<0.05.